

## Spatial shrinkage/expansion patterns between breast density measured in two MRI scans evaluated by non-rigid registration

This article has been downloaded from IOPscience. Please scroll down to see the full text article.

2011 Phys. Med. Biol. 56 5865

(<http://iopscience.iop.org/0031-9155/56/18/006>)

View [the table of contents for this issue](#), or go to the [journal homepage](#) for more

Download details:

IP Address: 128.200.55.216

The article was downloaded on 23/08/2011 at 21:47

Please note that [terms and conditions apply](#).

## Spatial shrinkage/expansion patterns between breast density measured in two MRI scans evaluated by non-rigid registration

Muqing Lin<sup>1</sup>, Jeon-Hor Chen<sup>1,2</sup>, Rita S Mehta<sup>3</sup>, Shadfar Bahri<sup>1</sup>,  
Siwa Chan<sup>4</sup>, Orhan Nalcioglu<sup>1,5</sup> and Min-Ying Su<sup>1,6</sup>

<sup>1</sup> Tu & Yuen Center for Functional Onco-Imaging, Department of Radiological Sciences, University of California, Irvine, CA, USA

<sup>2</sup> Department of Radiology, China Medical University Hospital, Taichung, Taiwan

<sup>3</sup> Department of Medicine, University of California, Irvine, CA, USA

<sup>4</sup> Department of Radiology, Taichung Veterans General Hospital, Taichung, Taiwan

<sup>5</sup> Department of Cogno-Mechatronics Engineering, Pusan National University, Korea

E-mail: [msu@uci.edu](mailto:msu@uci.edu)

Received 6 May 2011, in final form 5 July 2011

Published 18 August 2011


Online at [stacks.iop.org/PMB/56/5865](http://stacks.iop.org/PMB/56/5865)

### Abstract

Breast MRI acquires many images from the breast, and computer-aided algorithms and display tools are often used to assist the radiologist's interpretation. Women with lifetime risk greater than 20% of developing breast cancer are recommended to receive annual screening MRI, but the current breast MRI computer-aided-diagnosis systems do not provide the necessary function for comparison of images acquired at different times. The purpose of this work was to develop registration methods for evaluating the spatial change pattern of fibroglandular tissue between two breast MRI scans of the same woman taken at different times. The registration method is based on rigid alignment followed by a non-rigid Demons algorithm. The method was tested on three different subjects who had different degrees of changes in the fibroglandular tissue, including two patients who showed different spatial shrinkage patterns after receiving neoadjuvant chemotherapy before surgery, and one control case from a normal volunteer. Based on the transformation matrix, the collapse of multiple voxels on the baseline images to one voxel on the follow-up images is used to calculate the shrinkage factor. Conversely, based on the reverse transformation matrix the expansion factor can be calculated. The shrinkage/expansion factor, the deformation magnitude and direction, as well as the Jacobian determinate at each location can be displayed in a 3D rendering view to show the spatial changes between two MRI scans. These different parameters show consistent results and can be used for quantitative evaluation of the spatial change patterns. The presented registration method can be further developed into a clinical tool

<sup>6</sup> Author to whom any correspondence should be addressed.

for evaluating therapy-induced changes and for early diagnosis of breast cancer in screening MRI.

 Online supplementary data available from [stacks.iop.org/PMB/56/5865/mmedia](https://stacks.iop.org/PMB/56/5865/mmedia)

(Some figures in this article are in colour only in the electronic version)

## 1. Introduction

Screening mammography is the standard clinical examination for detecting early breast cancer. The radiologist reviews the mammogram of a woman by comparing it side-by-side with her previous mammogram (typically taken 1–2 years ago), so that the changes in breast density and/or micro-calcifications can be evaluated for detecting the growth of abnormal lesions. But mammograms do not work well in women with dense breasts, and in 2007 the American Cancer Society recommended that women with lifetime risk greater than 20% should receive annual breast MRI for screening (Saslow *et al* 2007). Since MRI acquires 3D images, more sophisticated image analysis algorithms and display tools are needed. It would be very helpful to develop a co-registration method so that the current MRI can be compared with the previous MRI done 1 year ago, similar to evaluation of mammograms for cancer detection.

If there is no enhanced lesion that is clearly visible, the changes in fibroglandular tissue (commonly referred to as the breast density) may provide useful information to aid in the detection of subtle abnormal changes, so that these areas can be followed more closely. However, the distribution of breast density is not uniform; thus, the capability to map out local changes within the entire breast is required. The current research in MRI-based density studies has been mainly focused on volumetric measurements of density in the whole breast (Klifa *et al* 2004, Nie *et al* 2008, Wei *et al* 2004). Unfortunately, the measurement of the total volume is too coarse and cannot be used for detecting local changes.

The evaluation of the spatial pattern of changes between two MRIs taken at different times may be accomplished by registration. In breast MRI, the enhanced lesion can be best visualized in subtraction images generated by subtracting pre-contrast from post-contrast images. However, due to the minor movement of the patient between these two acquisitions, subtraction artifacts are often seen, and the registration techniques are commonly applied to align images acquired before and after contrast injection (Rohlfing and Maurer 2003, Rueckert *et al* 1999). For the small changes between images acquired during the same scan session, rigid registration using the Affine transformation algorithm is sufficient. For registration of images taken at different scan sessions that has substantial change, non-rigid registration algorithms are required (Roose *et al* 2008). The method has been applied to co-register breast images acquired at prone and supine positions, so that the lesion detected on breast MRI in the prone position can be better utilized during the operation while the patient is lying at the supine position (Carter *et al* 2006, 2008). These previous studies have been for registration based on the boundary of the whole breast. The registration of the segmented fibroglandular tissue inside the breast has never been reported before.

In this work, we developed a method based on a non-rigid Demons registration algorithm to register the fibroglandular tissues acquired in two scans from the same woman. Based on the correspondence between two volumes, a metrics indicating the shrinkage/expansion of pixels within the breast was calculated. A three-dimensional rendering software was developed to display the changes in the breast from different views. The method was tested in three

**Table 1.** The total fibroglandular tissue volume measured in the baseline and the follow-up MRI studies, and the percentage change.

	Age	Baseline	Follow-up	Percent change
Subject 1 (chemotherapy patient)	32	190 (cm <sup>3</sup> )	116 (cm <sup>3</sup> )	39%
Subject 2 (chemotherapy patient)	41	116 (cm <sup>3</sup> )	110 (cm <sup>3</sup> )	5.2%
Subject 3 (normal volunteer)	36	36.6 (cm <sup>3</sup> )	35.9 (cm <sup>3</sup> )	1.9%

different subjects who had different degrees of changes in the fibroglandular tissue, including two patients who showed different spatial shrinkage patterns after receiving neoadjuvant chemotherapy before surgery, and one control case from a normal volunteer. This method will provide the basic framework upon which other algorithms (e.g. the matching of breast boundary) can be further developed and integrated in the future for detection of early cancer.

## 2. Materials and methods

### 2.1. Subjects and MR imaging protocol

The MRI of two patients (32 and 41 years old) who received neoadjuvant chemotherapy and had a baseline scan and a post-therapy scan after 3 months of treatment was analyzed. One normal volunteer (36 years old) who had two scans done 1 week apart was analyzed as a control case for comparison. The MRI was performed on a 3T Achieva system (Philips Medical Systems, Best, The Netherlands) using a dedicated breast coil. The non-fat-suppressed images acquired before injection of contrast agents were used for segmentation of the breast from the body, and segmentation of the fibroglandular tissue within the breast. The images were acquired using a 3D gradient-echo sequence in axial view to cover bilateral breasts. The parameters were as follows: FOV = 31–36 cm, image matrix 480 × 480, TR/TE = 6.2/1.26 ms, flip angle = 12°, and SENSE-factor = 2. Therefore, the in-plane resolution was 0.65–0.75 mm/pixel and the slice thickness was 2 mm.

### 2.2. Breast and fibroglandular tissue segmentation

The detailed procedures have been described in previous publications (Nie *et al* 2008, 2010). Briefly, a horizontal line was drawn through the posterior boundary of the sternum and all tissues below this line were considered as non-breast tissues and removed. The breast region was extracted using the fuzzy C-means (FCM)-based method and the chest wall muscle was identified using the B-spline curve fitting. The inhomogeneity of the signal intensity over the imaging field was corrected using an improved bias field correction algorithm (Lin *et al* 2011) based on combined N3 (Sled *et al* 1998) and FCM (Chen and Giger 2004). Then, the FCM algorithm was used to segment the fibroglandular and fatty tissues. The final segmentation results were visually verified by an experienced radiologist. For each subject, the procedure was applied to segment the fibroglandular tissues at the baseline and the follow-up studies independently, and the segmented 3D tissue structures obtained in the two studies were registered to evaluate the differences between them. The segmented fibroglandular tissue volume in the baseline and the follow-up studies, and the percentage change, are summarized in table 1.

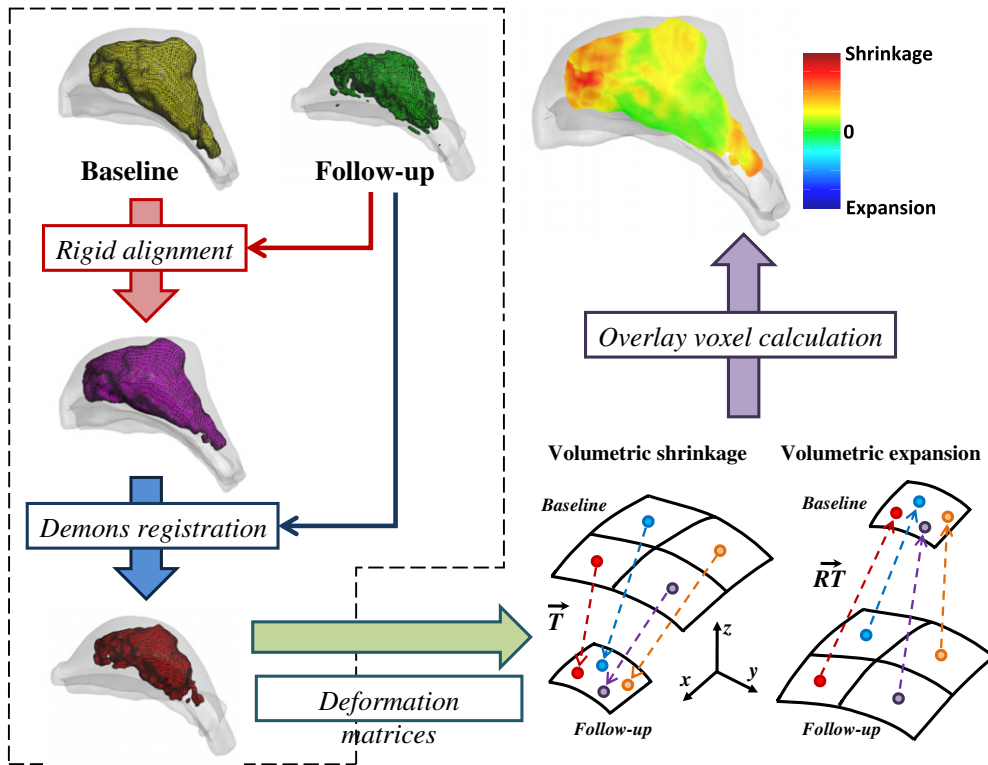


**Figure 1.** The overall registration procedures and the evaluation of local shrinkage/expansion based on the deformation matrix  $T$ . The segmented density in the pre-treatment baseline and post-therapy follow-up studies is first aligned with rigid translation and rotation. Then, the non-rigid Demons algorithm is used to register the baseline images (as the source) to match the follow-up images (as the target). The spatial shrinkage pattern is analyzed by calculating the convergence of multiple voxels on the source image into one voxel on the target image. For example, if four voxels ( $x_1, x_2, x_3$  and  $x_4$ ) in the source image collapse into the same voxel  $x_0$  in the target image, that indicates shrinkage with a shrinkage factor of three voxels. Expansion is analyzed based on the reverse transformation matrix  $RT$  from the target image to the source image using the same criteria. Lastly, the obtained shrinkage/expansion factor at each voxel location is color-coded and displayed on the baseline image.

### 2.3. Image registration

The overall registration procedures and the evaluation of local change based on deformation are shown in figure 1. The segmented density in pre-treatment baseline (B/L) and post-therapy follow-up (F/U) were first rigidly aligned based on six degrees of freedom, including three rotations ( $r_x, r_y, r_z$ ) and three translations ( $t_x, t_y, t_z$ ), using equation (1):

$$T_{\text{rigid}}(x, y, z) = \begin{pmatrix} r_x & r_y & r_z \end{pmatrix} \begin{pmatrix} x \\ y \\ z \end{pmatrix} + \begin{pmatrix} t_x \\ t_y \\ t_z \end{pmatrix}. \quad (1)$$

Let  $F$  be the fixed image (F/U),  $M$  be the moving image (B/L) and  $\circ$  be image transformation; the rigid alignment is the iterative process of minimizing the energy function  $E$ :

$$E_{\text{rigid}} = \|F - (T_{\text{rigid}} \circ M)\|. \quad (2)$$

The optimization of rigid transform was done using Powell's algorithm (Press *et al* 2002). After the global alignment, the Demons algorithm (Kroon and Slump 2009, Thirion 1998) was applied to locally match the density in B/L and F/U. Similar to (2), the energy function of the Demons algorithm is provided by

$$E(u) = \|F - M \circ (T + u)\|^2 + \sigma_n^2 |F - M|^2 \|u\|^2, \quad (3)$$

where  $T$  is the deformation field,  $u$  is the update for  $T$  in each iteration and  $\sigma_n$  is the image noise ratio coefficient. Let  $\nabla$  be the gradient of image and solve  $u$  by minimizing  $E$  to be 0; the estimated displacement of the original Demons algorithm (Thirion 1998) is given by

$$u = \frac{(M - F) \nabla F}{|\nabla F|^2 + (M - F)^2}. \quad (4)$$

In order to improve the speed of registration convergence and stability, the image edge force of the moving image (Wang *et al* 2005) is introduced to (4). The estimated displacement is now given by

$$u = \frac{(M - F) \nabla F}{|\nabla F|^2 + \alpha^2 (M - F)^2} + \frac{(M - F) \nabla M}{|\nabla M|^2 + \alpha^2 (M - F)^2}, \quad (5)$$

where  $\alpha$  is a constant which reduces the influence of edges (and noise) and limits the update speed of the transformation field.  $T$  is often initialized as zero (no displacement) while  $\sigma_n = 1/\alpha$  and  $\alpha = 0.6$  in our study. The Demons registration was done following these iterative processes.

- (a) Given  $T$ , update the new estimated displacement  $u$  by (5).  $u$  is further smoothed by a Gaussian kernel (with  $\sigma = 8$ ) for a fluid-like regulation.
- (b) Update  $T$  with the newly calculated  $u$  by  $T + u$ .  $T$  is further smoothed by a Gaussian kernel for a diffusion-like regulation (with  $\sigma = 1$ ).
- (c) Calculate a new cost function  $E$  based on the new deformation field.
- (d) If the difference of  $E$  between two consecutive iterations is less than a pre-set threshold ( $t = 0.0001$ ) or the registration process reaches the maximum iteration number ( $n = 200$ ), the iterative registration process is finished; otherwise, go back to step (a).

We adopted the version developed by Kroon and Slump (2009) that is available at <http://www.mathworks.com/matlabcentral/fileexchange/21451-multimodality-non-rigid-demon-algorithm-image-registration>.

#### 2.4. Evaluation of deformation

Based on the deformation matrix  $T$ , one can assess the spatial shrinkage pattern by analyzing the convergence of multiple voxels on the source image  $M$  into one voxel on the target image  $F$ , as illustrated in figure 1. For example, if four voxels ( $x_1, x_2, x_3$  and  $x_4$ ) in the source image collapse into the same voxel  $x_0$  in the target image after transformation ( $x_1 + T_1 \equiv x_2 + T_2 \equiv x_3 + T_3 \equiv x_4 + T_4 \equiv x_0$ ), that indicates shrinkage. Let  $\Omega(x)$  be the number of overlapping voxels; we have  $\Omega(x_1) = \Omega(x_2) = \Omega(x_3) = \Omega(x_4) = 4$ . A higher number of overlapping voxels indicate a greater shrinkage in this area. Expansion is analyzed based on the reverse transformation matrix  $RT$  using the same criteria from the target image to the source image. The shrinkage/expansion factor can be calculated by  $O(x) = \text{direction} \cdot (\Omega(x) - 1)$ , where  $\text{direction} = 1$  if shrinkage and  $\text{direction} = -1$  if expansion. The  $O(x)$  map was smoothed by the Gaussian kernel and color-coded to illustrate the spatial shrinkage/expansion patterns.

In addition to calculating the number of overlapping voxels, the Jacobian determinant of the deformation matrix was also used to evaluate the shape changes. This is a

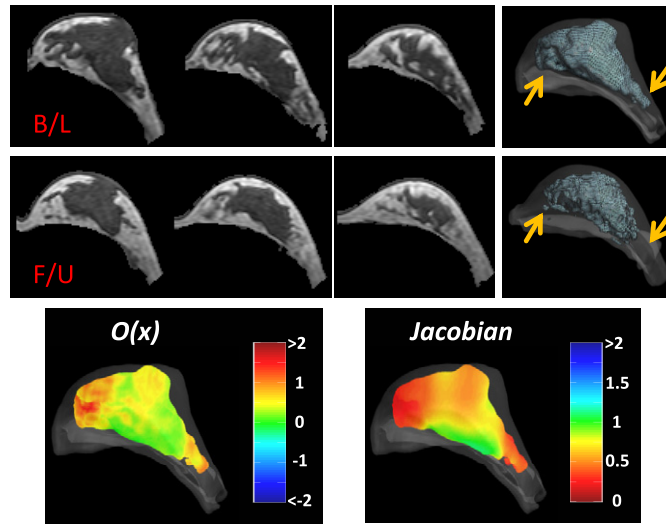


**Figure 2.** Comparison of fibroglandular tissues before (baseline, B/L) and after chemotherapy (follow-up, F/U) in the younger 32 year old patient. She has extremely dense breast at baseline and shows a severe atrophy after receiving chemotherapy. The total fibroglandular tissue volume decreases from 190 to 116 cm<sup>3</sup>. The most noticeable shrinkage is seen in the medial and the lateral sides, as marked by arrows. The map of the overlapping factor shows warm colors (orange to red) in the medial and lateral sides, indicating large shrinkage in these areas. In addition, the Jacobian determinant of the deformation matrix is used to evaluate the changes. For display purposes, the color bar is adjusted to show inward shrinkage ( $|J| < 1$ ) as warm colors and outward expansion ( $|J| > 1$ ) as cold colors. The Jacobian map is consistent with the map of the overlapping factor, also showing shrinkage in the medial and lateral sides.

common approach to assess the volumetric deformation (Qiu *et al* 2008). We adopted the implementation from the Insight Segmentation and Registration Toolkit (ITK, Ibanez *et al* 2005) and the Jacobian determinant is given by

$$|J| = \begin{vmatrix} 1 + 0.5 \cdot \frac{\partial T_x}{\partial x} & 0.5 \cdot \frac{\partial T_x}{\partial y} & 0.5 \cdot \frac{\partial T_x}{\partial z} \\ 0.5 \cdot \frac{\partial T_y}{\partial x} & 1 + 0.5 \cdot \frac{\partial T_y}{\partial y} & 0.5 \cdot \frac{\partial T_y}{\partial z} \\ 0.5 \cdot \frac{\partial T_z}{\partial x} & 0.5 \cdot \frac{\partial T_z}{\partial y} & 1 + 0.5 \cdot \frac{\partial T_z}{\partial z} \end{vmatrix}. \quad (6)$$

$|J| < 1$  indicates inward shrinkage, while  $|J| > 1$  indicates outward expansion.

### 3. Results

The methods are applied to three case examples. Figure 2 shows the younger chemotherapy patient (32 years old) who had extremely dense breasts at baseline and shows severe fibroglandular tissue atrophy after receiving chemotherapy. The total fibroglandular tissue volume was 190 cm<sup>3</sup> before treatment, and decreased to 116 cm<sup>3</sup> at the follow-up scan, showing 39% reduction. The shrinkage of breast density can easily be observed by visual inspection of the MR images, and the most noticeable changes are in the medial and the lateral sides. It can be seen that many voxels in the medial side of the breast show a shrinkage factor

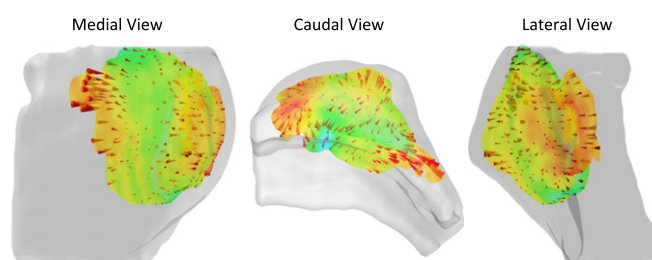


**Figure 3.** Illustration using the cone plot to indicate the amplitude and the direction of the deformation for voxels on the baseline image to match the follow-up image. The medial, caudal and lateral views are shown. This is the same case example shown in figure 2. Most deformations are pointing inward, indicating shrinkage. The results are consistent with the map of overlapping factors. The larger inward cones are seen in the warm color area with a higher shrinkage factor.

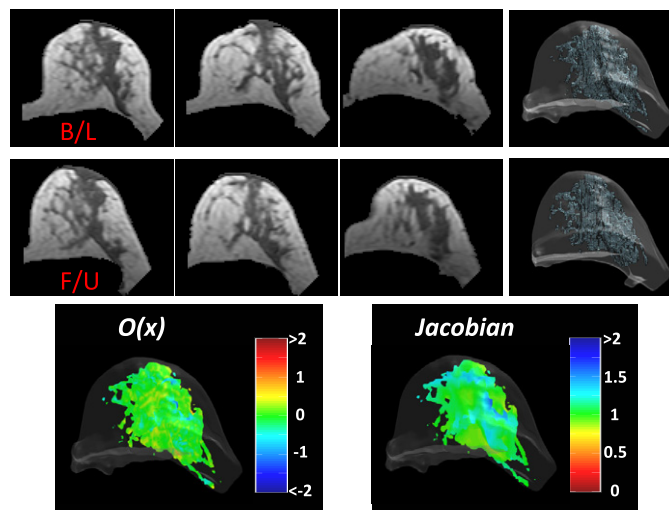
of greater than 2 (that is, more than three voxels on the baseline image collapse into one voxel on the follow-up image). A 3D rendering movie of the spatial shrinkage pattern is provided as a supplementary file (movie 1) available at [stacks.iop.org/PMB/56/5865/mmedia](https://stacks.iop.org/PMB/56/5865/mmedia). Figure 3 illustrates the difference in the breast density between the baseline and follow-up images by overlaying the cone plots from three different views (medial, caudal and lateral). The cones show the deformation amplitude and direction of pixels at each location on the baseline image to match the follow-up image. Most deformations are pointing inward, indicating shrinkage. The results are consistent with the map of overlapping factors. A 3D rendering movie of the overlay cone plot along the medial–lateral direction is provided as a supplementary file (movie 2) available at [stacks.iop.org/PMB/56/5865/mmedia](https://stacks.iop.org/PMB/56/5865/mmedia).

Figure 4 shows the results analyzed from the older chemotherapy patient (41 years old) who had a moderate breast density before treatment and showed milder atrophy compared to the younger patient. She also showed reduced fibroglandular tissue volume from 116 cm<sup>3</sup> at baseline to 110 cm<sup>3</sup> at follow-up, with 5.2% reduction. On the spatial shrinkage map, it can be seen that only a few voxels have overlapping factors greater than 1 (coded by yellow to orange color). Figure 5 shows the change in a healthy volunteer between two MRI scans acquired 1 week apart. The fibroglandular tissue volume was 36.6 cm<sup>3</sup> at baseline and 35.9 cm<sup>3</sup> at follow-up, only showing 1.9% difference. The spatial map of overlapping voxels was mostly coded by green, and the results indicate that there was very little change.

#### 4. Discussion and future works

In this work, we applied the non-rigid Demons algorithm to coregister breast densities between two scans taken at different times, and demonstrated that the number of collapsing voxels (noted as the shrinkage factor) at each spatial location during transformation can be used to illustrate the spatial shrinkage pattern. The results were consistent with the quantitative analysis of volumetric reduction and visual inspection findings. In the three selected case examples, the tool reveals the different atrophy patterns caused by chemotherapy, and shows very little change between two scans of a normal volunteer. The results suggest that this registration-based method can be used to provide information on the spatial change in breast density for visual inspection, also providing quantitative parameters using the shrinkage/expansion factor and the Jacobian determinant for further analysis of the degree of change. For cases





**Figure 4.** The results analyzed from the older chemotherapy patient (41 years old) who has a moderate breast density before treatment and shows milder atrophy after chemotherapy compared to the younger patient (from  $116 \text{ cm}^3$  at baseline to  $110 \text{ cm}^3$  at follow-up). Only a few voxels have a shrinkage factor greater than 1, showing as yellow to orange in color.

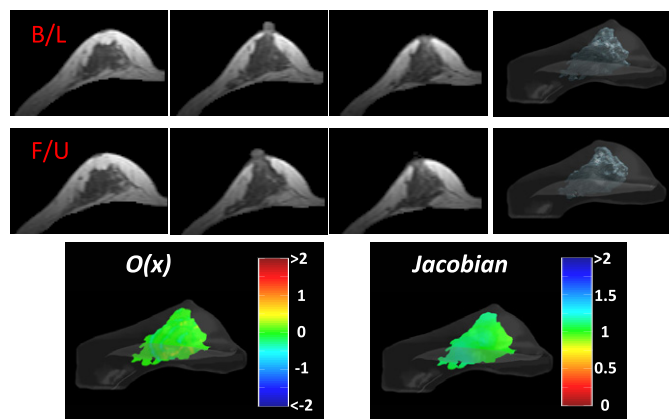


**Figure 5.** The changes between two MRI scans acquired from a healthy volunteer 1 week apart. The fibroglandular tissue volume is  $36.6 \text{ cm}^3$  at baseline, and  $35.9 \text{ cm}^3$  at follow-up. The map of the overlapping factor is mostly coded by green, indicating very little change.

that show substantial changes (e.g. subject 1), visual inspection can easily detect these changes. If a quantitative parameter is needed for any purpose (e.g. to correlate the change with patient's future recurrent cancer risk), the coarse volumetric measurement is probably sufficient. However, for cases with little change (e.g. subjects 2 and 3), these small changes cannot be detected by visual inspection, and the spatial pattern evaluated using the algorithms developed in this work might provide additional information.

The observed difference in the fibroglandular tissue mainly comes from two sources: the positioning difference of the breast between the two scans, and the intrinsic change of the

fibroglandular tissue within the breast. In theory, we can use both the outer boundary of the breast as well as the inner boundary of the fibroglandular tissue for registration, but this is a much more complicated problem and it will also be difficult to verify the obtained results. Therefore, as the initial approach, we selected three cases that show similar shapes of the breast between two scans, so that we can focus on registration of the fibroglandular tissue within the breast.

Given the highly deformable nature of soft breast tissue, MR scans of the same breast at different imaging sessions often present different shapes. In this case, traditional non-rigid registration methods may not be sufficient to recover the large deformations. Carter *et al* (2006, 2008) have successfully combined non-rigid registration together with the finite element model (FEM) to overcome the large deformation from two different scanning positions (e.g. between prone and supine). In the future, FEM-based registration may be applied as the pre-processing step to first match the shape of the breast (Cash *et al* 2005), before non-rigid registration is applied to co-register the fibroglandular tissue.

In the implementation of the Demons registration, the additive update of the transformation field ( $T + u$ ) was applied. Vercauteren *et al* (2009) suggested that the additive Demons algorithm is not fully diffeomorphic and may be incapable of matching objects with large curvature. They proposed a new exponential compositive Demons algorithm with the transformation field updated by  $T \circ \exp(u)$  that is fully diffeomorphic and has the potential to coregister objects with irregular boundaries. Whether the registration of the fibroglandular tissue can be further improved by this method needs to be evaluated.

In a recent paper, we demonstrated that the normal contralateral breast of patients receiving chemotherapy showed reduction of breast density (Chen *et al* 2010). Since the changes were different between pre-menopausal and post-menopausal patients, the results suggested that the reduction was mediated through the compromised ovarian function. The ability to analyze spatial change patterns may provide quantitative information for evaluating the chemotherapy-induced breast atrophy, as well as how it is related to changes in hormones and patient's future prognosis. In a very recent paper by Cuzick *et al* (2011), the change of breast density was shown as a surrogate marker to predict the efficacy in patients receiving tamoxifen as a chemopreventive drug to reduce the risk of developing breast cancer. Measurement of breast density on mammography is not reliable (Kopans 2008), and the presented method in this work may provide a useful tool and new imaging biomarkers for evaluating the efficacy of cancer therapy or chemoprevention.

Another important application of this method is for comparing annual screening MRI in high-risk women to evaluate whether there are any regions showing significant changes in density. If an increase of density is found in a specific region by comparing it to the prior scan, this patient may need close follow-up to monitor the development of abnormal lesions. For detecting such a small localized change, we need high precision, and all possible reasons that may cause spatial difference of the breast between two scans (including the positioning) need to be considered. As the next task, we will develop the registration of the breast boundary using the finite-element-based method, so that the positioning difference can be eliminated, and then we can proceed with the fibroglandular tissue registration according to the method presented in this work.

In summary, we proposed a new method for evaluating the spatial change pattern of fibroglandular tissue between two breast MR scans of the same woman at different times. The deformation analyzed using the combined rigid and non-rigid registration methods can be used to evaluate the collapse of voxels in one volume to match the other, thus indicating the shrinkage, and vice versa for expansion. The Jacobian, as well as the magnitude and direction of the deformation, can be displayed in a 3D rendering view. However, the method

was only tested in three cases, for proof of feasibility, and further evaluation in more cases is needed. The presented method in this paper will provide the basic framework upon which other algorithms (e.g. the matching of breast boundary) can be further developed and integrated. These methods can be developed into a clinical tool for evaluating the therapy-induced changes and for early diagnosis of breast cancer in screening MRI.

## Acknowledgments

This work was supported in part by NIH R01 CA127927, R03 CA136071, California BCRP 14GB-0148, 16GB-0056 and DMR-99-062 from the China Medical University Hospital in Taiwan. This study was conducted at the Center for Functional Onco-Imaging, University of California, Irvine.

## References

- Carter T, Tanner C, Beechey-Newman N, Barratt D and Hawkes D 2008 MR navigated breast surgery: method and initial clinical experience *Med. Image Comput. Comput. Assist. Interv.* **11** 356–63
- Carter T J, Tanner C, Crum W R, Beechey-Newman N and Hawkes D J 2006 A framework for image-guided breast surgery *Medical Imaging Augmented Reality (MIAR)* vol 4091 pp 203–10
- Cash D M, Miga M I, Sinha T K, Galloway R L and Chapman W C 2005 Compensating for intraoperative soft-tissue deformations using incomplete surface data and finite elements *IEEE Trans. Med. Imaging* **24** 1479–91
- Chen J H, Nie K, Bahri S, Hsu C C, Hsu F T, Shih H N, Lin M, Nalcioglu O and Su M Y 2010 Decrease in breast density in the contralateral normal breast of patients receiving neoadjuvant chemotherapy: MR imaging evaluation *Radiology* **255** 44–52
- Chen W and Giger M L 2004 A fuzzy c-means (FCM) based algorithm for intensity inhomogeneity correction and segmentation of MR images *IEEE Int. Symp. on Biomedical Imaging (ISBI '04)* vol 2 pp 1307–10
- Cuzick J, Warwick J, Pinney E, Duffy S W, Cawthorn S, Howell A, Forbes J F and Warren R M 2011 Tamoxifen-induced reduction in mammographic density and breast cancer risk reduction: a nested case-control study *J. Natl Cancer Inst.* **103** 744–52
- Klifa C, Carballido-Gamio J, Wilmes L, Laprie A, Lobo C, Demicco E, Watkins M, Shepherd J, Gibbs J and Hylton N 2004 Quantification of breast tissue index from MR data using fuzzy cluster *Conf. Proc. IEEE Eng. Med. Biol. Soc.* vol 3 pp 1667–70
- Kopans D B 2008 Basic physics and doubts about relationship between mammographically determined tissue density and breast cancer risk *Radiology* **246** 348–53
- Kroon D J and Slump C H 2009 MRI modality transformation in demon registration *IEEE Int. Symp. on Biomedical Imaging (ISBI '09)* pp 963–66
- Ibanez L, Schroeder W, Ng L and Cates J 2005 *The ITK Software Guide* 2nd edn (Albany, NY: Kitware)
- Lin M, Chan S, Chen J H, Chang D, Nie K, Chen S T, Lin C J, Shih T C, Nalcioglu O and Su M Y 2011 A new bias field correction method combining N3 and FCM for improved segmentation of breast density on MRI *Med. Phys.* **38** 5–14
- Nie K, Chang D, Chen J H, Shih T C, Hsu C C, Nalcioglu O and Su M Y 2010 Impact of skin removal on quantitative measurement of breast density using MRI *Med. Phys.* **37** 227–33
- Nie K, Chen J H, Chan S, Chau M K, Yu H J, Bahri S, Tseng T, Nalcioglu O and Su M Y 2008 Development of a quantitative method for analysis of breast density based on three-dimensional breast MRI *Med. Phys.* **35** 5253–62
- Press W H, Teukolsky S A, Vetterling W T and Flannery B P 2002 *Numerical Recipes in C* 2nd edn ed L Cowles, A Harvey and R Hahn (New York: Cambridge University Press) pp 412–20
- Qiu A, Younes L, Miller M I and Csernansky J G 2008 Parallel transport in diffeomorphisms distinguishes the time-dependent pattern of hippocampal surface deformation due to healthy aging and the dementia of the Alzheimer's type *Neuroimage* **40** 68–76
- Rohlfing T and Maurer C R 2003 Volume-preserving nonrigid registration of MR breast images using free-form deformation with an incompressibility constraint *IEEE Trans. Med. Imaging* **22** 730–41
- Roose L, Loeckx D, Mollemans W, Maest F and Suetens P 2008 Adaptive boundary conditions for physically based follow-up breast MR image registration *Med. Image Comput. Comput. Assist. Interv.* **11** 839–46

- Rueckert D, Sonoda L I, Hayes C, Hill D L, Leach M O and Hawkes D J 1999 Nonrigid registration using free-form deformations: application to breast MR images *IEEE Trans. Med. Imaging* **18** 712–21
- Saslow D *et al* American Cancer Society Breast Cancer Advisory Group 2007 American Cancer Society guidelines for breast screening with MRI as an adjunct to mammography *CA Cancer J. Clin.* **57** 75–89
- Sled J G, Zijdenbos A P and Evans A C 1998 A nonparametric method for automatic correction of intensity nonuniformity in MRI data *IEEE Trans. Med. Imaging* **17** 87–97
- Thirion J P 1998 Image matching as a diffusion process: an analogy with Maxwell's Demons *Med. Image Anal.* **2** 243–60
- Wang H, Dong L, O'Daniel J, Mohan R, Garden A S, Ang K K, Kuban D A, Bonnen J Y, Chang M and Cheung R 2005 Validation of an accelerated 'Demons' algorithm for deformable image registration in radiation therapy *Phys. Med. Biol.* **50** 2887–905
- Wei J, Chan H P, Helvie M A, Roubidoux M A, Sahiner B, Hadjiiski L M, Zhou C, Paquerault S, Chenevert T and Goodsitt M M 2004 Correlation between mammographic density and volumetric fibroglandular tissue estimated on breast MR images *Med. Phys.* **31** 933–42
- Vercauteren T, Pennec X, Perchant A and Ayache N 2009 Diffeomorphic Demons: efficient non-parametric image registration *Neuroimage* **45** 61–72